Catal Lett (2012) 142:547–556
DOI 10.1007/s10562-012-0807-3

Modeling of Temperature-Programmed Desorption (TPD) Flow Experiments from $Cu/ZnO/Al_2O_3$ Catalysts

M. Peter · J. Fendt · H. Wilmer · O. Hinrichsen

Received: 1 March 2012 / Accepted: 11 March 2012 / Published online: 3 April 2012

Abstract Different procedures to extract the kinetics of hydrogen desorption from a $Cu/ZnO/Al_2O_3$ catalyst for methanol synthesis were studied by performing temperature-programmed desorption experiments under atmospheric pressure. The four methods include (i) heating rate variation, (ii) analysis using a fixed pre-exponential factor, (iii) lineshape analysis and (iv) full analysis. Before extracting the parameters, transport limitations could be excluded for all experiments and a criterion for inner particle mass transfer limitations could be extended in the case of activated re-adsorption. All methods could be valid in the whole range of experiments, with only one exception for the lineshape analysis at full coverage of hydrogen. However, each method requires different input to extract physically meaningful parameters. The best modeling results were obtained when repulsive interactions of adsorbed species were accounted for. This led to a $k_{des} = 3.75{\cdot}10^{10}\ s^{-1}{\cdot}\exp(-(75\ kJ{\cdot}mol^{-1} - 5.5\ kJ{\cdot}mol^{-1}{\cdot}\Theta_H^{2.6})/RT)$ in good agreement with the literature. Moreover, it was found that there is no difference, when extracting the kinetic parameters from a fresh or deactivated catalyst at full coverage.

Keywords $Cu/ZnO/Al_2O_3$ catalyst · Hydrogen temperature-programmed desorption (H_2 TPD) · Microkinetic analysis · Lineshape analysis · Heating rate variation

M. Peter · J. Fendt · O. Hinrichsen (✉)
Catalysis Research Center and Chemistry Department, Technische Universität München, 85748, Garching b. München, Germany
e-mail: olaf.hinrichsen@ch.tum.de

H. Wilmer
BASF SE, Carl-Bosch-Straße 38, 67056 Ludwigshafen, Germany

List of Symbols

Variables

A_{ads}	Arrhenius factor of adsorption $(Pa\ s)^{-1}$
A_{des}	Arrhenius factor of desorption (s^{-1})
c_{H_2}	Concentration of hydrogen $(mol\ m^{-3})$
D_{ax}	Axial dispersion coefficient $(m^2\ s^{-1})$
D_e	Effective diffusion coefficient $(m^2\ s^{-1})$
E_{ads}	Activation energy of adsorption $(kJ\ mol^{-1})$
E_{des}	Activation energy of desorption $(kJ\ mol^{-1})$
K	Factor of coverage-dependent activation energy $(kJ\ mol^{-1})$
k_{ads}	Reaction rate constant of adsorption $(Pa\ s)^{-1}$
k_{des}	Reaction rate constant of desorption (s^{-1})
L	Length of reactor bed (m)
n	Power of coverage-dependent activation energy (–)
$N_{H_2,sat}$	Saturation coverage of hydrogen $(mol\ kg^{-1})$
P_{H_2}	Partial pressure of hydrogen (Pa)
Q	Flow rate $(Nml\ min^{-1})$
R	Ideal gas constant $(J\ mol^{-1}K^{-1})$
r_p	Radius of catalyst particle (m)
$S_{critical}$	Value for criterion (–)
T	Temperature (K)
t	Time (s)
T_{max}	Temperature at peak maximum (K)
u	Superficial velocity $(m\ s^{-1})$
w_{cat}	Catalyst weight (g)
X_{ref}	Reference value (mol–%)
x	Dimensionless reactor coordinate (–)
z	Dimensionless particle coordinate (–)

Greek Symbols

β	Heating rate $(K\ min^{-1})$
ε_b	Bed porosity (–)

ε_p Particle porosity (–)
γ Source term (mol m^{-3} s^{-1})
Θ_H Degree of coverage (of hydrogen) (–)
ρ_p Particle density (kg m^{-3})
τ Residence time (s)

1 Introduction

Temperature-programmed techniques are widely used in surface science studies in order to extract kinetic parameters. Routinely, thermal desorption spectroscopy (TDS) under ultra-high vacuum (UHV) conditions is applied to determine kinetic information from well-defined single crystals. This is a straightforward way to analyze the kinetic properties, since effects like re-adsorption or mass transfer limitations are negligible [1]. However, such well-defined surfaces and ideal conditions may have a lack of applicability to working conditions due to the big pressure and material gaps. Modern flow set-ups work under ambient pressure and are suited for studying microkinetics (in terms of elementary steps) on porous catalysts close to reaction conditions [2, 3]. In particular, concentration-programmed experiments, e.g. pulse and step function or switch experiments, and temperature-programmed flow experiments, e.g. performed as TP desorption (TPD) or adsorption (TPA) experiment, are frequently used in microkinetic studies of heterogeneously catalyzed gas-phase reactions [4–6].

In general, several mathematical procedures exist for the evaluation of kinetic parameters of temperature-programmed experiments, resulting in terms of Arrhenius parameters for the rate constants, i.e. A_{ads}, A_{des}, E_{ads}, E_{des}. In general, the methods can be divided into two groups: (a) the integral approach which relates the kinetic parameters to desorption characteristics such as full width at half maximum (FWHM) and temperatures at peak maximum; (b) differential analyses of the desorption spectra resulting in pairs of desorption rate/temperature. While the integral approach is applied to extract coverage-independent kinetic parameters, differential techniques are used to obtain a coverage-dependence of the kinetic parameters.

In order to test different approaches to extract kinetic parameters, hydrogen desorption from Cu-based ternary ($Cu/ZnO/Al_2O_3$) catalysts employed in methanol synthesis was studied. This has been a subject of great interest during the last decade [7–13]. It was clearly demonstrated that hydrogen recombinatively desorbs from copper surface sites. Furthermore, these metallic copper sites have been identified as the active sites for methanol synthesis [14, 15]. From UHV studies it is known that hydrogen adsorption on copper single crystals proceeds via dissociation and is regarded to be highly activated. Similarly, this was demonstrated also for ternary copper catalyst [10, 11, 16–19]. Since re-adsorption is less or even negligible when adsorption is a highly activated process, interpretation of the flow TP desorption data are less demanding and desorption can be studied separately. Simple transient experiments such as the variation of the heating rate at constant initial coverage have been carried out to determine the desorption kinetics in detail followed also by a simple evaluation method to describe the desorption process in term of Arrhenius parameters [8, 11]. However, more advanced methods can be applied, which, in turn, require experimental TPD spectra obtained with different initial coverages at the same heating rate [7, 10]. The determination of the kinetic parameters was not the only subject of interest. Muhler et al. [9] developed a method to determine the copper surface area of binary Cu/Al_2O_3 and ternary $Cu/ZnO/Al_2O_3$ catalysts via H_2 TPD flow experiments, which is, compared to the widely used N_2O frontal chromatography [20, 21], non destructive. Wilmer et al. [11, 12] studied the interaction of hydrogen with ZnO-containing copper and Cu/Al_2O_3 catalysts in detail. They found that a pretreatment in a mild atmosphere (He) prior to hydrogen desorption experiments leads to almost similar kinetic values for the catalysts, indicating that there is only a slight influence by ZnO on the copper sites and Al_2O_3 mainly acting as a structural promoter. However when changing the pretreatment procedure to more severe conditions, in particular to a pretreatment with carbon monoxide, hydrogen desorption spectra change in shape and peak positions. Experiments indicate morphology changes or even surface alloying under highly reducing conditions [11, 12].

In previous flow TPD studies, only coverage-independent desorption parameters assuming ideal Langmuirian behavior were extracted for modeling the interaction of hydrogen with Cu-based catalysts employed in methanol synthesis [8, 11]. In general, this approach results in modeled signals being too narrow at full coverage. The reason for that is mainly due to neglecting adsorbate–adsorbate and adsorbate–substrate interactions [11]. Moreover, diffusion limitations could possibly broaden the signals measured at the reactor outlet flow. In this study a valuable criterion for diffusion limitations was adapted and reconsidered in the case of activated re-adsorption [22]. This work compares different methods to receive kinetic parameters from TPD experiments. It is shown that numerical methods such as non linear least-squares fitting can describe TPD experiments more adequately than the present evaluation of heating rate variation, while using physical meaningful input parameters from experimental analysis. A coverage-dependent activation energy leads to even better results than previously extracted ones neglecting a coverage-dependence.

2 Experimental and Computational Section

In our study, the H_2 TPD experiments were carried out in a completely glass-coated stainless steel set-up. Only gases of high purity (>99.9995 %) were used. Fast on-line analysis of the gas components was achieved by a calibrated quadrupole mass spectrometer (Balzers GAM 422). The H_2 TPD experiments were measured using an industrial $Cu/ZnO/Al_2O_3$ catalyst, of which 200 mg (sieve fraction 250–355 μm) were filled into a single-pass fixed-bed reactor. Details on the set-up can be found elsewhere [8, 23].

In order to achieve different hydrogen coverages Θ_H, on the one hand the dosing temperature can be varied; on the other hand the dosing duration might be varied. In addition to these two experimental procedures the H_2 TPD experiments can be stopped at different temperatures to achieve the desired hydrogen coverage. This was achieved by quenching the outside of the reactor with liquid N_2. Subsequently a second temperature ramp was initialized. Using this method, the desired coverages can be obtained very exactly. Comparison of this procedure with the ones mentioned before showed only negligible differences [8, 23].

The results for the heating rate variations were taken from previous work by Wilmer et al. [11]. Prior to the TPD experiments methanol synthesis was performed over night. This procedure led to a reduced number of active sites. This evidence will be discussed later in more detail.

The fixed bed reactor was modeled as a continuously stirred-tank reactor (CSTR), a plug flow reactor (PFR) and a convection-axial dispersion reactor model (C-ADR), respectively. Also intraparticle mass transfer was investigated. The governing equations for the CSTR, PFR and C-ADR are given as [22]:

$$\frac{dc_{H_2}}{dt} = -\frac{1}{\tau(t)} c_{H_2} + \gamma$$

$$\frac{dc_{H_2}}{dt} = -\frac{u(t)}{L\varepsilon_b}\frac{dc_{H_2}}{dx} + \gamma$$

$$\frac{dc_{H_2}}{dt} = \frac{D_{ax}}{L^2\varepsilon_b}\frac{d^2c_{H_2}}{dx^2} - \frac{u(t)}{L\varepsilon_b}\frac{dc_{H_2}}{dx} + \gamma$$

where γ without intraparticle mass transfer is defined as:

$$\gamma = \frac{(1-\varepsilon_b)\rho_p N_{H_2,sat}}{\varepsilon_b} \cdot \left(-\frac{d\theta_H}{dt}\right)$$

and

$$\gamma_{IPMT} = -\frac{3D_e(1-\varepsilon_b)}{r_p^2\varepsilon_b} \cdot \frac{dc_{H_2}}{dz}\bigg|_{z=1}$$

when considering intraparticle mass transfer. The corresponding particle balance is given by:

$$\frac{dc_{H_2}}{dt} = \frac{D_e}{r_p^2\varepsilon_p}\left(\frac{d^2c_{H_2}}{dz^2} + \frac{2}{z}\frac{dc_{H_2}}{dz}\right) + \frac{\rho_p N_{H_2,sat}}{\varepsilon_p} \cdot \left(-\frac{d\theta_H}{dt}\right)$$

A time-dependent balance for adsorbed species was used, assuming a one-step mechanism, as there is no evidence for molecularly adsorbed hydrogen from experiments on Cu surfaces:

$$H_2 + 2* \rightleftharpoons 2H*$$

The corresponding differential equation yields:

$$\frac{d\theta_H}{dt} = 2 \cdot \left(k_{ads} p_{H_2}(1-\theta_H)^2 - k_{des}\theta_H^2\right)$$

Differential equations were solved with a sparse system adaptive ODE solver "ode15s", using Mathworks Inc. MATLAB® R2009b. Tolerances were set to a value of 10^{-8}. Partial differential equations were discretized by the method of lines [24]. For the models without inner particle mass transfer at least 100 equidistant grid points and for all other models 40 grid points in reactor and particle coordinate were used. Backward differences were used to describe the reactor system. Second order derivatives, i.e. diffusion related, were calculated by a central difference scheme. All spectra were tested against numerical convergence and mass conservation. For fittings, the MATLAB® non linear least-squares fitting function "lsqnonlin" was implemented. The termination tolerance on the function value was chosen to be 10^{-15}. Detection by a quadrupole mass spectrometer provides very sensitive data analysis. Consequently, a thorough data reduction was applied for further modeling aspects. A well defined temperature interval was chosen, containing all relevant information, i.e. from the onset to the ending of the signal of hydrogen. In order to reduce the experimental noise the number of data points was decreased by a factor of 20. Besides this, the position of the signal maxima is also included to the objective function. An alternative way of data reduction is a fit around the desorption maximum.

The rate constants k_i were modeled in Arrhenius form. For rate constants concerning the recombinative desorption of hydrogen, both a coverage-dependent and coverage-independent approach was used. In our notation k_{des} is reported in s^{-1}, including the condition that one active site is represented by two copper surface atoms [8, 11, 25]. The coverage-dependent form can account for repulsive and attractive interactions of adsorbed molecules, since the assumption of Langmuirian desorption may be not adequate at high or low coverage.

In order to compare different spectra, a dimensionless scaled root mean square error between the experimental value f_1 and the modeling result f_2 is used:

$$\mathrm{SRMSE} = \frac{1}{X_{\mathrm{ref}}}\sqrt{\frac{1}{N}\sum_{\mathrm{j}=1}^{\mathrm{N}}\left(f_1(j) - f_2(j)\right)^2}$$

The root mean square error is divided by a reference value X_{ref}. The reference value was chosen in the following way: when comparing two simulations the higher mole fraction of hydrogen at the temperature maximum was used, while the experimental value was chosen when comparing simulation with experiment. For SRMSE values below 0.045 two responses are considered to be equal, within experimental uncertainty [22].

3 Results

3.1 Mass Transfer Limitations

Most of the common techniques to determine kinetic parameters are only applicable when transfer limitations such as inner particle mass transfer or re-adsorption as a specific phenomenon occurring in porous systems can be excluded. Wilmer et al. [11] analyzed the dissociative adsorption of hydrogen via temperature-programmed adsorption experiments. They found an activation energy of $E_{\mathrm{ads}} = 48$ kJ mol^{-1} and an Arrhenius factor of $A_{\mathrm{ads}} = 6{\cdot}10^2$ (Pa s)$^{-1}$. Comparing modeling results with this set of kinetic parameters with respect to results of a model without re-adsorption leads to a SRMSE value of about $4{\cdot}10^{-3}$. When adsorption is chosen to be less activated re-adsorption becomes evidently significant. Figure 1 shows the modeled traces of hydrogen desorption for different values of A_{ads} and E_{ads}. Changing the activation energy of adsorption to a value of 40 kJ mol^{-1}

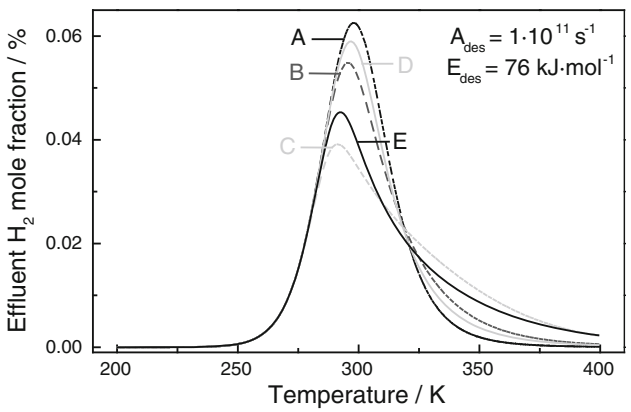

Fig. 1 Modeled H_2 TPD spectra with different Arrhenius adsorption parameters: (*A*) $A_{\mathrm{ads}} = 6{\cdot}10^2$ (Pa s)$^{-1}$, $E_{\mathrm{ads}} = 48$ kJ·mol^{-1}, (*B*) $A_{\mathrm{ads}} = 6{\cdot}10^2$ (Pa s)$^{-1}$, $E_{\mathrm{ads}} = 40$ kJ·mol^{-1}, (*C*) $A_{\mathrm{ads}} = 6{\cdot}10^2$ (Pa s)$^{-1}$, $E_{\mathrm{ads}} = 35$ kJ·mol^{-1}, (*D*) $A_{\mathrm{ads}} = 6{\cdot}10^3$ (Pa s)$^{-1}$, $E_{\mathrm{ads}} = 48$ kJ·mol^{-1}, (*E*) $A_{\mathrm{ads}} = 6{\cdot}10^4$ (Pa s)$^{-1}$, $E_{\mathrm{ads}} = 48$ kJ·mol^{-1}, experimental conditions: $Q_{\mathrm{He}} = 100$ Nml·min^{-1}, $\beta = 6$ K·min^{-1}, $w_{\mathrm{cat}} = 0.2$ g, $\Theta_{\mathrm{H}} = 1$

significantly broadens the signal behind the temperature of the signal maximum (T_{max}). For values below 41 kJ mol^{-1} re-adsorption becomes relevant (SRMSE > 0.045). Lowering the activation energy to 35 kJ mol^{-1} makes the signal highly asymmetric. The less activated re-adsorption is, the higher is the shift of T_{max} towards lower temperatures. Changes in A_{ads} have a lower influence on the significance of re-adsorption. A value of $A_{\mathrm{ads}} = 6{\cdot}10^3$ (Pa s)$^{-1}$, which is one magnitude higher than the initial value, has still an SRMSE value below $3{\cdot}10^{-2}$. However raising the Arrhenius factor by another magnitude makes re-adsorption significant and the shift of T_{max} is about 4 K. Since there is no broadening of the measured TPD signals is observed re-adsorption can be excluded, which is also indicated by the low SRMSE value.

Besides re-adsorption, intraparticle diffusion limitations always have to be considered for porous catalysts. However, H_2 TPD experiments are usually performed under conditions where heat and mass transport limitations are negligible [8, 11]. A lot of criteria exist for testing for intraparticle mass transfer limitations, mainly dealing with simplifications [26–29]. Recently, Kanervo et al. [22] established a criterion, which is easily accessible by applying the following formula:

$$\frac{1/\tau}{D_{\mathrm{e}}/r_{\mathrm{p}}^2} = \frac{\mathrm{Q}r_{\mathrm{p}}^2\rho_{\mathrm{p}}(1-\varepsilon_{\mathrm{b}})}{D_{\mathrm{e}}w_{\mathrm{cat}}\varepsilon_{\mathrm{b}}} < S_{\mathrm{critical}}$$

This criterion can be interpreted as the ratio of convective to diffusive flow. High flow rates have to be compensated by a high catalyst mass or by a low particle radius in order to avoid intraparticle mass transfer limitations. Kanervo et al. [22] gave an overview of relevant parameters for TPD flow reactor models. Their criterion was tested against these parameters by relaxing one of the controllable parameters, namely Q, w_{cat} or r_{p}, at a time, keeping the rest constant. When S_{critical} is below 0.16 a TPD experiment can safely be described by a plug flow reactor.

However, testing our experimental values against this criterion within the range of Knudsen and effective molecular diffusion led to values that should show significant intraparticle mass transfer limitations. For our set of parameters, values for S_{critical} were obtained in the range from 0.03 to 0.76. This would imply that one has to account for mass transfer phenomena. Nevertheless, no significant differences between a model with and without intraparticle mass transfer can be observed, when modeling these regimes in case of the hydrogen desorption and using the kinetic values taken from Wilmer et al. [11] (Fig. 2), with $E_{\mathrm{ads}} = 48$ kJ mol^{-1}, $E_{\mathrm{des}} = 76$ kJ mol^{-1} and Arrhenius factors of $A_{\mathrm{ads}} = 6{\cdot}10^2$ (Pa s)$^{-1}$ and $A_{\mathrm{des}} = 10^{11}$ s^{-1}. Comparing a model with and without intraparticle mass

transfer, a SRMSE value of $5{\cdot}10^{-3}$ is obtained, which means intraparticle mass transfer limitation can be neglected. Furthermore, comparing the two diffusion regimes, Knudsen and effective molecular diffusion, yields an SRMSE value below $3{\cdot}10^{-4}$ (not shown in Fig. 2). As being derived for our set of parameters intraparticle mass transfer can be excluded. Consequently, the criterion can be enlarged to $S_{\text{critical}} < 40$ when re-adsorption is a significantly activated process. This is achieved by varying the parameters of the criterion equation appropriately until the SRMSE value reaches the critical value of 0.045, when comparing the models.

Axial dispersion accounts for back mixing in a fixed bed reactor. Additionally, Fig. 2 shows the influence of axial dispersion using an axial dispersion coefficient calculated from the given criterion equation with a reasonable value of 2 for the Peclet number [30]. The limiting cases for $\text{Pe} \rightarrow 0$ and $\text{Pe} \rightarrow \infty$ are considered by using a CSTR or PFR model, respectively. Comparing a PFR with and without axial dispersion, one obtains completely negligible deviations, as being displayed in Fig. 2 and validated by an SRMSE value below $5{\cdot}10^{-5}$. Furthermore, modeling the TPD using a CSTR reactor model, the respective signal of hydrogen in the outlet flow is mathematically identical to the models mentioned before, leading to SRMSE $< 5{\cdot}10^{-3}$.

3.2 Determination of Kinetic Parameters

In order to determine the kinetic parameters of the H_2 desorption from Cu surface sites, four mathematical procedures were applied. The results were taken to model the flow temperature-programmed desorption experiments at different initial coverages of hydrogen. These methods comprise of (i) heating rate variation, (ii) analysis using a fixed pre-exponential factor, (iii) lineshape analysis and (iv) full model fitting. In general, all methods require different experimental input. The use of the heating rate variation needs data obtained from experimental TPD flow response curves using several heating rates [4, 5, 8, 11]. Typically, the experiments are performed for the initial coverage of a monolayer. Mathematical analysis leads to one pair of corresponding values for A_{des} and E_{des}. According to the method of Redhead [31] the pre-exponential factor A_{des} is kept constant at 10^{13} s^{-1}, yielding an overall value for the activation energy of desorption E_{des} for every spectrum. Each evaluated spectrum can yield a different activation energy of desorption at a single heating rate or initial coverage. Although the Redhead's peak maximum method was derived for evaluation of first order desorption kinetics under UHV conditions, it is straightforward to apply an analogous approach for second order desorption (recombinative desorption) using a model fit with a pre-exponential factor fixed at $1{\cdot}10^{13}$ s^{-1}. Additionally, a lineshape analysis method was used to fit the TPD spectra [10]. This procedure was also referred as "Arrhenius plots" [4] and can be applied to a single TPD spectrum. It results in pairs of values for A_{des} and E_{des} for every experiment. Finally, a nonlinear least-squares fit to a single TPD response is used to find the desired parameters, including a coverage-dependence. This approach promises to find kinetic parameters valid for the whole spectrum of recorded TPD experiments. In the following all methods are presented in more detail.

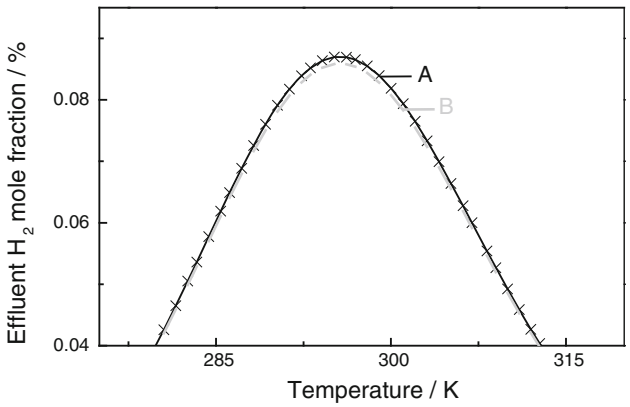

Fig. 2 Modeled H_2 TPD spectra with different reactor models: (*A*) plug flow reactor, (*B*) plug flow reactor with intraparticle mass transfer, (×) represents results for a plug flow reactor with axial dispersion, enlarged excerpt around the desorption maxima, experimental conditions: $Q_{\text{He}} = 100$ Nml min^{-1}, $\beta = 6$ K min^{-1}, $w_{\text{cat}} = 0.2$ g, $\Theta_{\text{H}} = 1$

In an earlier publication [11], the kinetic parameters of the hydrogen desorption from Cu-based catalysts were determined from the experimental TPD flow experiments applying different heating rates at full coverage. Full coverage ($\Theta_{\text{H}} = 1$) is thereby considered as a monolayer of adsorbed hydrogen. The maximum of the desorption signal is shifted to higher temperatures with rising heating rate, while the onset of the signals remains at the same temperature of approximately 240 K. Using Langmuirian second order desorption kinetics with negligible re-adsorption, the signal shift could be analyzed quantitatively. A plot of $\ln(T_{\text{max}}^2/\beta)$ against $1/T_{\text{max}}$ yielded the activation energy of the desorption E_{des} of 76 ± 2 kJ mol^{-1} and a pre-exponential factor A_{des} of $1{\cdot}10^{11} \pm 2{\cdot}10^{11}$ s^{-1} [11]. The modeling results for each heating rate, displayed in Fig. 3, showed that the heating rate variation is a reliable tool that fits the experimental data comparatively well, however, with deviations at high coverage. As mentioned before, this is due to the fact that the assumption of a Langmuirian desorption is not adequate for high coverages. Figure 4 shows the experimental data and simulation results for different hydrogen coverages obtained with a fresh catalyst (not deactivated). Simulated spectra are generated with kinetic parameters extracted

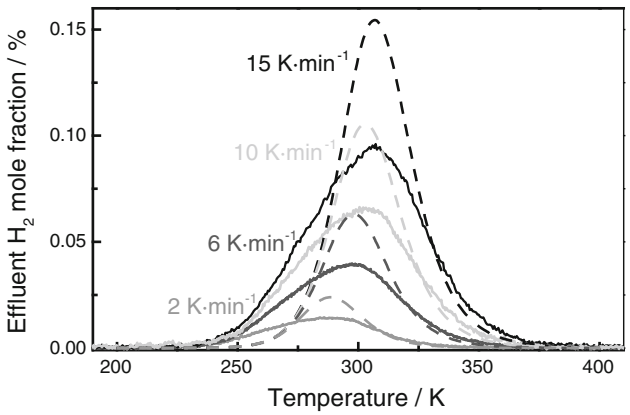

Fig. 3 Heating rate variation, $A_{des} = 1{\cdot}10^{11}$ s^{-1}, $E_{des} = 76$ kJ mol^{-1}, kinetic values taken from [11]: Experimental H_2 TPD spectra (*solid lines*) and simulated curves (*dashed lines*), experimental conditions: $Q_{He} = 100$ Nml min^{-1}, $w_{cat} = 0.2$ g, $\Theta_H = 1$

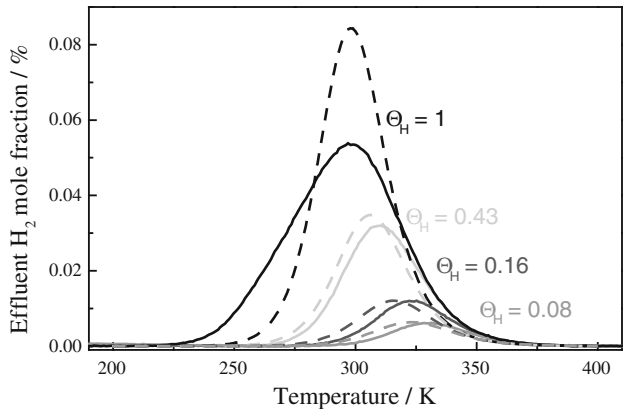

Fig. 4 Hydrogen coverage variation, $A_{des} = 1{\cdot}10^{11}$ s^{-1}, $E_{des} = 76$ kJ mol^{-1}, kinetic values taken from [11]: Experimental H_2 TPD spectra (*solid lines*) and simulated curves (*dashed lines*), experimental conditions: $Q_{He} = 100$ Nml min^{-1}, $w_{cat} = 0.2$ g, $\beta = 6$ K min^{-1}

from the heating rate variation experiments [11]. For smaller coverages a shift in T_{max} towards higher temperatures can be observed, whereby the descending signal curves approximate. This is due to the fact that adsorbed molecules have fewer neighbors at lower coverages. For the associative desorption a reactive collision has to take place. For lower coverages such a collision is less probable. Furthermore, the onsets of the signals are at different temperatures. Only at full coverage the repulsive interaction of the hydrogen atoms becomes important, which can clearly be seen by the widening of the signal. At full coverage of hydrogen, the simulated signal is too narrow again (see also Fig. 3), whereas at lower coverages the shapes of the signals can be reproduced sufficiently exact. However the shift in the onset and of maximum temperature is underestimated by the kinetic parameters obtained from the heating rate experiments.

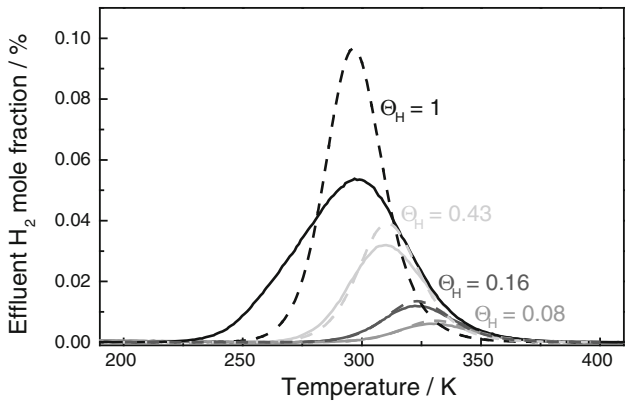

Fig. 5 Hydrogen coverage variation, modeling according to fixed pre-exponential factor analysis, $A_{des} = 1{\cdot}10^{13}$ s^{-1}, $E_{des} = 86$–90 kJ mol^{-1}: Experimental H_2 TPD spectra (*solid lines*) and simulated curves (*dashed lines*), experimental conditions: $Q_{He} = 100$ Nml min^{-1}, $w_{cat} = 0.2$ g, $\beta = 6$ K min^{-1}

Modeling results based on a model fit with a fixed pre-exponential factor at $1{\cdot}10^{13}$ s^{-1} are shown in Fig. 5. Values for E_{des} of 86.5, 88.7, 89.8 and 90.2 ± 1 kJ mol^{-1} have been extracted for coverages of $\Theta_H = 1$, 0.43, 0.16 and 0.08, respectively. By this procedure the activation energy is independent from the Arrhenius factor and no compensation effects between the pre-exponential factor and the energy of desorption are possible. The activation energy depends on the temperature at peak maximum and the initial coverage. That means the activation energy increases with lower coverages, as the signals shift to higher temperatures. Interestingly, an analysis according to Redhead [31], assuming the same pre-exponential factor of $1{\cdot}10^{13}$ s^{-1}, leads to very similar values for the activation energies (±0.5 kJ mol^{-1}), even for the second order desorption considered here. When comparing the modeled signals, the results are comparable to the ones of the heating rate variation with less deviation at lower coverages (Fig. 5) according to the SRMSE values. The T_{max} values are reproduced better though.

Furthermore, a particularly good fit of the respective experimental spectra (Fig. 6) is achieved by the lineshape analysis method [4, 10], resulting in pairs of A_{des} and E_{des} for each spectrum (Table 1). Plots of $\ln(r_{des}/\Theta_H^2)$ against $1/T$ for different initial coverages leads to a straight line. The rate of desorption is proportional to the height of the peak at that temperature, whereas the area behind that peak is equivalent to the coverage of hydrogen at that rate. Intercept and slope yield the desired parameters, A_{des} and E_{des}, respectively. However, this method results in unreasonable physical values, i.e. A_{des} ranging from $1.8{\cdot}10^7 \pm 2{\cdot}10^7$ to $6{\cdot}10^{13} \pm 6{\cdot}10^{13}$ s^{-1} and E_{des} ranging from 54 to 95 ± 3 kJ mol^{-1}.

Since transport limitations could be excluded and all simulated signals at high coverage are narrower than the

corresponding experimental ones, a fourth approach was introduced in order to reproduce the experimental data more adequately. The Langmuirian assumption seems to be not adequately enough, the coverage-dependence was introduced into the energy of desorption as follows:

$$E_{\mathrm{des}}(\theta_{\mathrm{H}}) = E_{\mathrm{des}}(\theta_{\mathrm{H}} = 0) - \mathrm{K}\theta_{\mathrm{H}}^{\mathrm{n}}$$

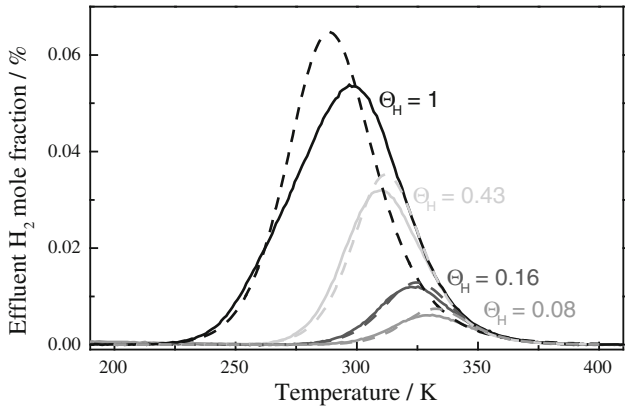

Fig. 6 Lineshape analysis $A_{\mathrm{des}} = 1.8{\cdot}10^{7}{-}6{\cdot}10^{13}$ s^{-1}, $E_{\mathrm{des}} = 54{-}95$ kJ mol^{-1}: Experimental H_2 TPD spectra (*solid lines*) and simulated curves (*dashed lines*), experimental conditions: $Q_{\mathrm{He}} = 100$ Nml min^{-1}, $w_{\mathrm{cat}} = 0.2$ g, $\beta = 6$ K min^{-1}

The models are fitted to the experimental results using a nonlinear least-squares fit, which requires an initial guess. As a starting point, the physically meaningful results of the heating rate variation were chosen, which can be interpreted as mean values. One experimental response was chosen ($\Theta_{\mathrm{H}} = 1$, $\beta = 6$ K min^{-1}, fresh catalyst), all other spectra were simulated using the derived kinetic parameters. First, a fixed linear coverage-dependence was considered ($n = 1$), yielding $K = 5.5$ kJ mol^{-1}. The model description of the experiments improves significantly, however, the onset and the ending of the signal were not reproduced sufficiently, yielding a SRMSE value around 0.13. Nevertheless, a second order dependence further improves the description of the experiment. When the order of coverage-dependence n is finally relaxed, parameters are obtained which reproduce the experiments very accurately. The results of the kinetic parameters are well in the range of reference values [7, 8, 10, 11, 25], i.e. the best fit for a heating rate of 6 K min^{-1} is obtained for $A_{\mathrm{des}} = 3.75{\cdot}10^{10} \pm 4{\cdot}10^{10}$ s^{-1} and $E_{\mathrm{des}} = 75 \pm 3$ kJ·mol$^{-1}{-}5.5 \pm 1.5$ kJ·mol$^{-1}{\cdot}\Theta_{\mathrm{H}}^{2.6\ \pm\ 0.4}$. Again, it has to be pointed out that the fitting was performed with the data taken from one specific TPD experiment, where both ways of data reduction yielded essentially the same results. The validity of the model parameters is indicated by the means that only one experimental spectrum is sufficient to extract the desired

Table 1 Parameters derived from different methods, results for the heating rate variation are taken from Wilmer et al. [11]

Figure	Method	Θ_{H}^{-}	β K min^{-1}	A_{des} s^{-1}	E_{des} kJ mol^{-1}	SRMSE –
3	Heating rate variation	1	2	$1.00{\cdot}10^{11}$	76.00	0.228
3	Heating rate variation	1	6	$1.00{\cdot}10^{11}$	76.00	0.214
3	Heating rate variation	1	10	$1.00{\cdot}10^{11}$	76.00	0.219
3	Heating rate variation	1	15	$1.00{\cdot}10^{11}$	76.00	0.210
4	Heating rate variation	1	6	$1.00{\cdot}10^{11}$	76.00	0.200
4	Heating rate variation	0.43	6	$1.00{\cdot}10^{11}$	76.00	0.082
4	Heating rate variation	0.16	6	$1.00{\cdot}10^{11}$	76.00	0.128
4	Heating rate variation	0.08	6	$1.00{\cdot}10^{11}$	76.00	0.127
5	Fixed prefactor	1	6	$1.00{\cdot}10^{13}$	86.54	0.255
5	Fixed prefactor	0.43	6	$1.00{\cdot}10^{13}$	88.72	0.067
5	Fixed prefactor	0.16	6	$1.00{\cdot}10^{13}$	89.75	0.040
5	Fixed prefactor	0.08	6	$1.00{\cdot}10^{13}$	90.16	0.061
6	Lineshape analysis	1	6	$1.80{\cdot}10^{7}$	53.60	0.139
6	Lineshape analysis	0.43	6	$3.00{\cdot}10^{11}$	80.30	0.044
6	Lineshape analysis	0.16	6	$2.20{\cdot}10^{12}$	86.30	0.036
6	Lineshape analysis	0.08	6	$6.00{\cdot}10^{13}$	95.40	0.084
7	Full analysis	1	6	$3.75{\cdot}10^{10}$	$74.95{-}5.51{\cdot}\Theta^{2.59}$	0.024
7	Full analysis	1	6	$3.75{\cdot}10^{10}$	$74.95{-}5.51{\cdot}\Theta^{2.59}$	0.031
7	Full analysis	0.43	6	$3.75{\cdot}10^{10}$	$74.95{-}5.51{\cdot}\Theta^{2.59}$	0.013
7	Full analysis	0.16	6	$3.75{\cdot}10^{10}$	$74.95{-}5.51{\cdot}\Theta^{2.59}$	0.035
7	Full analysis	0.08	6	$3.75{\cdot}10^{10}$	$74.95{-}5.51{\cdot}\Theta^{2.59}$	0.042

parameters. This approach allows to easily implement a coverage-dependent activation energy for desorption. Figure 7 shows the results for the fit when considering coverage-dependence (fresh catalyst at full coverage). The corresponding simulations at different hydrogen coverages as well as for a deactivated catalyst at full coverage ($\Theta_H = 1$, smaller peak height) are included here. It can clearly be seen that the coverage-dependence improves the mathematical model. It fits the data from other experiments in an excellent way with respect to the shape of the signal and to the position of T_{max}. Regarding all evaluation methods, the coverage-dependence becomes less important at lower coverages. For clarity, the spectra for the other heating rates (2, 10 and 15 K min^{-1}) are not shown in Fig. 7. The agreement between experimental and modeled spectra is also very good, leading to SRMSE values below 0.034.

4 Discussion

When interpreting temperature-programmed desorption flow experiments under ambient pressure care should be taken. Common techniques for UHV conditions are only valid when re-adsorption processes and transport limitations during the TPD flow experiments can be excluded. During those experiments, the concentration of the desorbing molecules is reduced by the dilution of the carrier gas. Thereby the re-adsorption probability is decreased. In our case, the absence of re-adsorption processes is confirmed by comparative simulations. However, it is clearly demonstrated that re-adsorption processes are highly sensitive on the desorption signal. Compared to the findings of Kanervo et al. [22], the absence of re-adsorption also enhances the mass transfer inside the particle and therefore minimizes the effect of intraparticle mass transfer, since re-adsorption becomes less when activated. For the criterion of Kanervo et al. [22], only extremely low activated re-adsorption (up to $E_{ads} = 10$ kJ mol^{-1}) was taken into account, resulting in a more rigorous value. When adsorption is a highly activated process only slight differences in the reactor models are observable (see also Fig. 2).

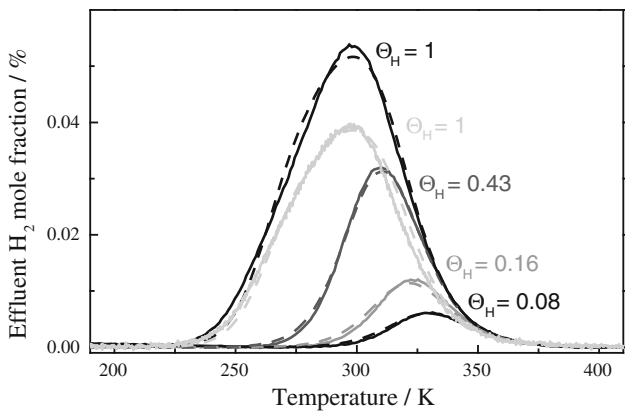

Fig. 7 Results for $A_{des} = 3.75{\cdot}10^{10}$ s^{-1}, $E_{des} = 75{-}5.5$ kJ mol$^{-1}{\cdot}\Theta_H{}^{2.6}$: Experimental H_2 TPD spectra (*solid lines*) and simulated curves (*dashed lines*), experimental conditions: $Q_{He} = 100$ Nml min^{-1}, $w_{cat} = 0.2$ g, $\beta = 6$ K min^{-1}

Since no transfer limitations are observable in our experiments, the determination of the desorption kinetics is straightforward. Table 1 summarizes all kinetic parameters determined by the different procedures, together with the calculated SRMSE values. The highest SRMSE values are obtained when modeling traces at full coverage. This is attributed to significant broadening of the experimental H_2 TPD spectra due to non-Langmuirian behavior for Θ_H towards 1. The results obtained by an analysis with a fixed pre-exponential factor demonstrate that the activation energy increases with lower coverage and desorption becomes more activated. The energy of desorption increases about 4 kJ mol^{-1} for a coverage from 1 to 0.08. Care should be taken when the data are discussed with a physical background and the pre-exponential factor is unknown and therefore chosen to be $1{\cdot}10^{13}$ s^{-1}. While Roberts and Griffin [32] found a comparable energy of desorption of about 86 kJ mol^{-1} utilizing the Redhead's peak maximum method, different methods, which also yield a pre-exponential factor, led to activation energies around 70 kJ mol^{-1} [8, 10, 11]. An appropriate choice of the pre-exponential factor is essential for the extraction of a physically meaningful value for E_{des}, i.e. choosing a pre-exponential factor of $1{\cdot}10^{11}$ s^{-1} leads to an E_{des} of around 75 kJ mol^{-1} for $\Theta_H = 1$. While heating rate variation yields mean values, this method covers the full range of coverage, assuring physically meaningful parameters for A_{des} and E_{des}. This can also be seen when comparing the results to those obtained by the lineshape analysis method, which are comparable at an intermediate coverage of $\Theta_H = 0.43$. However, the lineshape analysis method failed at full coverage, resulting in kinetic parameters which are not physically meaningful and in a position of T_{max} being completely wrong. For lower coverages, the compensation effect of A_{des} and E_{des} led to higher values for the respective parameter. Though, the agreement between experiment and simulation is high. For all methods the error becomes less when the coverage is lowered, except for the model fitting where all values are below 0.045. Accounting for the repulsive interaction of the hydrogen atoms by a factor of $5.5{\cdot}\Theta_H{}^{2.6}$ kJ mol^{-1} fits the experiments best. A full analysis yields $k_{des} = 3.75{\cdot}10^{10}$ s$^{-1}{\cdot}$exp (−(75 kJ·mol^{-1}−5.5 kJ·mol^{-1} $\Theta_H^{2.6}$)/RT), which is comparable for the results by Anger et al. [7] for Cu(111), suggesting that the catalysts predominantly exposes Cu(111) facets. This is in perfect agreement with results published in

previous studies [8, 10, 11]. A coverage-dependent Arrhenius factor of $3.4{\cdot}10^{10}$ to $1.5{\cdot}10^{11}$ s^{-1} and an activation energy of 63 to 77 kJ mol^{-1} was found based on the assumption that one active site consists of two copper surface atoms ($\Theta_{H,max} = 1$) [25]. On Cu(111), Anger et al. [7] extracted a coverage-dependent factor of the activation energy of $K = 14.6$ kJ mol^{-1}. However, in a previous work [25] it was already shown that this value was too high, overestimating the coverage-dependence. An analysis using a fixed pre-exponential factor led to an increase of about 4 kJ mol^{-1}, indicating that a value of $K = 5.5$ kJ mol^{-1} is in an absolutely reasonable magnitude. The factor of 2.6 is contributed to the shape of the signal and can therefore be interpreted as the magnitude of repulsive interactions of the adsorbed species. It should be pointed out that care should be taken when evaluating TPD data with model fits. An approach with a more rigorous and straightforward procedure comprises the following steps: simultaneously fitting of all parameters, searching for a global minimum and therefore the best mathematical description of the experiments. This procedure yields even a better fit (SRMSE of about 0.01). However, quite physically unlikely values of $A_{des} = 7{\cdot}10^{8}$ s^{-1} and E_{des} ranging from 57 to 62 kJ mol^{-1} were obtained. It is highly recommended to evaluate TPD experiments with common techniques, i.e. heating rate variation, before the model fitting.

An accurate explanation of hydrogen desorption is very relevant for microkinetic modeling in industrial processes, in particular, for the water gas shift and methanol synthesis reaction. Both reactions comprise of several hydrogenation steps over Cu-based catalysts. Microkinetic models have been introduced based on the surface science approach [33–39]. In particular, the change in morphology has been included using Wulff's construction, leading to a description of the rate of methanol formation in terms of the contributions of different Cu facets as a function of the atmosphere applied. With respect to our results for the deactivated and non-deactivated state of the catalyst, a comparison indicates that the morphology reversibly changes, since the obtained kinetic data are equal for both catalysts. For the results taken from Wilmer et al. [11] the ternary catalyst was deactivated by performing methanol synthesis at very mild conditions. Then, the catalyst was reduced and flushed with helium to achieve an adsorbate-free copper surface before the TPD experiment. It is remarkable that the experimental TPD traces of the deactivated and not deactivated catalyst (i.e. Fig. 7, $\Theta_H = 1$) do not show any differences in the onset or peak maximum temperature. This clearly means that deactivation of the catalyst only decrease the number of active sites, i.e. in our experiment by about 25 %. Obviously, the parameters can be determined using a fresh or deactivated catalyst in the same way.

5 Conclusions

A criterion by Kanervo et al. [22] was revised and enlarged in order to be applicable for highly activated adsorption processes during second order desorption experiments. When re-adsorption and transport limitations can be neglected within the experimental range, different analysis methods can be applied in order to extract kinetic parameters from TPD flow experiments. In the case of hydrogen desorption from a ternary Cu-based catalyst, parameters obtained by the heating rate variation and the lineshape analysis at an intermediate coverage of Θ_H are in a physically meaningful range. Care should be particularly taken for the lineshape analysis at full coverage, which could not even reproduce the position of T_{max}. An analysis with a fixed pre-exponential factor results in comparable values when the pre-exponential factor A_{des} is known. All methods are generally applicable to extract kinetic parameters from temperature-programmed flow desorption experiments, but care should be taken when repulsive interactions are not negligible. Nonetheless, sufficient experimental data should be used. Parameters from a single experiment, i.e. extracted by an analysis method using a fixed pre-exponential factor or the lineshape analysis, might not be significant or even physically unreasonable. A full analysis showed that the best results are obtained when the activation energy varies with coverage. The analysis led to $k_{des} = 3.75{\cdot}10^{10}$ $s^{-1}{\cdot}\exp(-(75\ kJ{\cdot}mol^{-1} - 5.5\ kJ{\cdot}mol^{-1}\ \Theta_H^{2.6})/RT)$. It is in a range, which is comparable to the values found before [7, 8, 10, 11], but describes all experiments more precisely.

For the simulations, the desorption spectra for the methods based on Langmuirian assumptions are essentially the same, however when this assumption is relaxed, a better agreement between experiment and simulation can be achieved. Hence, an exact description of the coverage-dependence on ternary catalysts enhances the detailed understanding of those reaction mechanisms at industrially more relevant conditions.

Acknowledgments Fruitful discussions with Martin Muhler are gratefully acknowledged.

References

1. Niemantsverdriet JW (2007) Spectroscopy in catalysis. Wiley-VCH, Weinheim
2. Dumesic JA, Rudd DF, Aparicio LM, Rekoske JE, Treviño AA (1993) The microkinetics of heterogeneous catalysis. ACS Professional Reference Book, Washington DC
3. Hinrichsen O (2008) In: Ertl G, Knözinger H, Schüth F, Weitkamp J (eds) Handbook of heterogeneous catalysis, vol 3. Wiley-VCH, Weinheim
4. de Jong AM, Niemantsverdriet JW (1990) Surf Sci 233:355
5. Falconer JL, Schwarz JA (1983) Catal Rev Sci Eng 25:141

6. Miller JB, Siddique HR, Gates SM, Russell JN Jr, Yates JT Jr, Tully JC, Cardillo MJ (1987) Chem Phys 87:6725
7. Anger G, Winkler A, Rendulic KD (1989) Surf Sci 220:1
8. Genger T, Hinrichsen O, Muhler M (1999) Catal Lett 59:137
9. Muhler M, Nielsen LP, Törnqvist E, Clausen BS, Topsøe H (1992) Catal Lett 14:241
10. Tabatabaei J, Sakakini BH, Watson MJ, Waugh KC (1999) Catal Lett 59:143
11. Wilmer H, Genger T, Hinrichsen O (2003) J Catal 215:188
12. Wilmer H, Hinrichsen O (2002) Catal Lett 82:117
13. Xia X, Strunk J, Litvinov S, Muhler M (2007) J Phys Chem C 111:6000
14. Chinchen GC, Waugh KC, Whan DA (1986) Appl Catal 25:101
15. Pan WX, Cao R, Roberts DL, Griffin GL (1988) J Catal 114:440
16. Campbell JM, Campbell CT (1991) Surf Sci 259:1
17. Hayden BE, Lackey D, Schott J (1990) Surf Sci 239:119
18. Hayden BE, Lamont CLA (1989) Chem Phys Lett 160:331
19. Hayden BE, Lamont CLA (1989) Phys Rev Lett 63:1823
20. Chinchen GC, Hay CM, Vanderwell HD, Waugh KC (1987) J Catal 103:79
21. Scholten JJF, Konvalinka JA (1969) Trans Faraday Soc 65:2465
22. Kanervo JM, Keskitalo TJ, Slioor RI, Krause AOI (2006) J Catal 238:382
23. Genger T (2000) Mikrokinetische Untersuchungen zur Methanol-Synthese an Cu-Trägerkatalysatoren. PhD thesis, Ruhr-Universität Bochum
24. Löwe A (2001) Chemische Reaktionstechnik. Wiley-VCH, Weinheim
25. Hinrichsen O, Rosowski F, Muhler M, Ertl G (1997) Stud Surf Sci Catal 109:389
26. Balkenende AR, Geus JW, Kock AJHM, van der Pas RJ (1989) J Catal 115:365
27. Demmin RA, Gorte RJ (1984) J Catal 90:32
28. Forzatti P, Tronconi E, Lietti L (1988) In: Cheremisinoff NP (ed) Handbook of heat and mass transfer, vol 3. Gulf Publishing Co., Houston
29. Rieck JS, Bell AT (1984) J Catal 85:143
30. Emig G, Klemm E (2005) Technische Chemie. Springer, Berlin
31. Redhead PA (1962) Vacuum 12:203
32. Roberts DL, Griffin GL (1988) J Catal 110:117
33. Rasmussen PB, Taylor PA, Chorkendorff I (1992) Surf Sci 269(270):352
34. Taylor PA, Rasmussen PB, Ovesen CV, Stoltze P, Chorkendorff I (1992) Surf Sci 261:191
35. Ovesen CV, Stoltze P, Nørskov JK, Campbell CT (1992) J Catal 134:445
36. Rasmussen PB, Holmblad PM, Askgaard T, Ovesen CV, Stoltze P, Nørskov JK, Chorkendorff I (1994) Catal Lett 26:373
37. Askgaard TS, Nørskov JK, Ovesen CV, Stoltze P (1995) J Catal 156:229
38. Ovesen CV, Clausen BS, Hammershøi BS, Steffensen G, Askgaard T, Chorkendorff I, Nørskov JK, Rasmussen PB, Stoltze P, Taylor P (1996) J Catal 158:170
39. Ovesen CV, Clausen BS, Schiøtz J, Stoltze P, Topsøe H, Nørskov JK (1997) J Catal 168:133